JOINT INSTITUTE FOR NUCLEAR RESEARCH
Dzhelepov Laboratory of Nuclear Problems

FINAL REPORT ON THE INTEREST PROGRAMME

Monte Carlo simulation of radiation-matter interaction for shielding evaluation in medical imaging applications

Supervisor:
Dr. Antonio Leyva Fabelo

Student:
Nikita Sochivko, Belarus
Belarusian State University

Participation period:
30 October – 10 December, Wave 9

Dubna, 2023

Contents

Abstract

The MCNP code system based on the Monte Carlo method will be used to simulate the interaction of radiation with matter, to study radiation shielding in a selected medical application: preclinical SPECT/CT scanner. The simulation will include the most important parts of the scanner with typical materials and dimensions. Some of the most widely used radioisotopes in SPECT imaging (^{201}Tl, ^{133}Xe, ^{99m}Tc, ^{133}I, etc.) will be used as gamma sources. Interesting will be the simulation in the CT geometry of a Roentgen X-ray tube emitting strictly with the characteristic spectrum that corresponds to the selected anode (W) and the tube operating parameters. Taking into consideration that the safe operation of the scanner by technical and medical personnel must comply with the radiation protection requirements demanded at international level, the calculated dose rates for different conditions will be compared with the limit values of safe dose rates established for each group of people. The results will be analyzed in detail in the project.

Keywords: Computed tomography, single photon emission tomography, Monte Carlo N-Particle Transport code.

Introduction

Since the introduction of computed tomography (CT) in the early 1970s, the rapid development of the technology and capabilities of these scanners has accelerated the implementation of many new clinical applications. One such advantage is the hybrid imaging SPECT/CT system, which is continuing to gain popularity in nuclear medicine and cardiology facilities. Combined SPECT/CT systems allow the sequential acquisition of anatomic and molecular data while minimizing changes in patient position, improving attenuation correction, and providing inherently coregistered anatomic images.

Although the technology clearly has its benefits, new developments in hybrid imaging technology, including combining SPECT with multislice CT systems, result in higher exposure levels for patients, a greater occupational hazard to staff from scattered radiation and the requirement for increased shielding in a nuclear medicine department. In general, effective dose for CT examinations can be higher than most other diagnostic imaging modalities. There is also a considerable choice of CT user-selectable exposure factors resulting in a significant variation in CT dose to the patient. This study aims to simulate radiation exposure associated with the SPECT/CT scanner, study radiation shielding with taking into consideration that the safe dose rates must comply with the radiation protection requirements demanded at International Commission on Radiation Protection with respect to minimizing the effective dose established for each group of people.

Project objectives

- Study of methods for mathematical modeling of radiation interaction with matter.
- Familiarization with SPECT and CT imaging techniques.
- Determination from literature of the safe exposure dose limits for occupationally exposed personnel and patients.
- Preparation or adjustment of the MCNP input files for the calculations, including the conversion of the obtained fluence data to dose rate units.
- Calculation by mathematical modeling of the dose rate spatial distribution in the experimental system for typical sources and different radiation protection conditions.

1 Materials and methods

1.1 SPECT/CT tomography

1.1.1 Computed tomography

X-ray computed tomography (CT) is an X-ray imaging technique that can non-destructively scan the density distribution of an object in 3D and reveal internal structures. It was developed in 1971 to axial imaging human brains in neuroradiology and has been widely used for medical purposes such as: oncology, vascular radiology, cardiology, traumatology and interventional radiology, for a good reason: it is non-destructive.

The resolution of the medical CT scanners is in the submillimeter to millimeter order because it uses a computer to process attenuation data acquired from the patient. These attenuation values, or their linear attenuation coefficients μ are subsequently converted into integers referred to as CT numbers and all values are normalized to the attenuation of water (μ_{water}). Attenuation values are captured by special detector system which convert electrical signals to digital data for processing. The computer uses a sophisticated mathematical process referred to as image reconstruction, which uses specialized algorithms to build up and display images of a patient's internal anatomy for diagnostic interpretation. CT images are essentially cross-sectional images of slices that are perpendicular to the long axis of the patient (multislice CT scanning (MSCT) on Fig. 1).

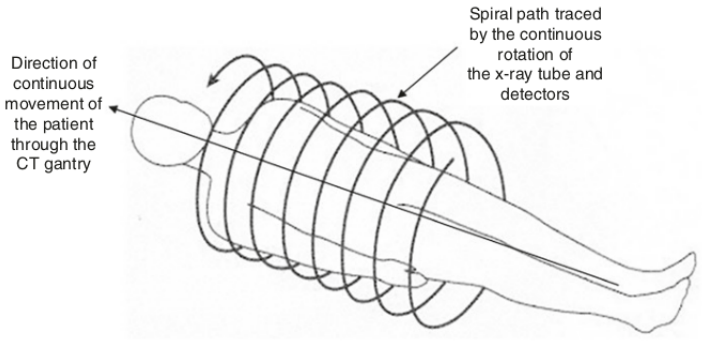

Figure 1. In MSCT scanning, the path traced by the X-ray beam as the patient moves through the gantry aperture during scanning and is called a spiral or helical path [1].

The major system components of a CT imaging are illustrated in Fig. 2. These consist of data acquisition; image reconstruction; and image display and storage. While data acquisition collects X-ray transmission readings by scanning the patient; image reconstruction uses these readings to build up a CT image of the patient's scanned anatomy. The transmitted radiation consists of attenuation values μ which are subsequently converted by the detector electronics into digital data for processing by a computer.

The data acquisition components of the CT scanner are: a X-ray tube, a beam shaping filter and pre-patient collimators. The X-ray tube is coupled to an array of detectors which collect radiation transmitted through the patient. The detectors send electrical signals to analog-to-digital converters (ADCs) which convert analog signals into digital data for processing by the CT host computer.

Image reconstruction in CT is based on sophisticated mathematics and has evolved from back projection to filtered back projection to more complex iterative reconstruction and currently artificial intelligence-based algorithms.

Image display and storage represent the third system component of the CT scanner. Images are displayed on a monitor for viewing and interpretation, and can be subject to post processing

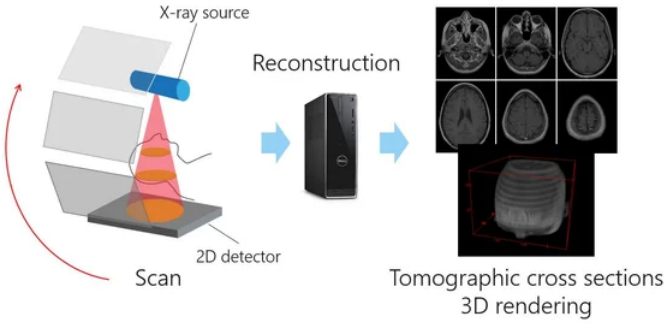

Figure 2. The major system components of a CT imaging [2].

to suit the viewing needs of the observer.

Radiation attenuation is defined as the reduction of the intensity of a beam of radiation as it passes through matter or the patient's body. Attenuation behaves differently for a homogeneous beam (all photons in the beam have the same energy) and for a heterogeneous beam (all photons have different energies). The original experiments in CT performed by Hounsfield used a homogeneous beam from Americium because this beam holds true for a law of attenuation referred to as Beer-Lambert Law, described by the equation:

$$I = I_0 \exp^{-\mu x}, \tag{1}$$

where I is the transmitted intensity; I_0 is the original intensity, μ is the linear attenuation coefficient, or the fractional reduction in the intensity of a beam of radiation per unit thickness of the medium traversed; and x is the thickness of the object.

Attenuation values are converted into CT numbers. The system normalizes all tissue attenuation values to the attenuation of water. CT numbers are computed using the following algebraic expression [1]:

$$CTNumber = \frac{\mu - \mu_{water}}{\mu_{water}} \cdot K, \tag{2}$$

where K is the scaling factor of the CT manufacturer. In general, K is equal to 1000. CT numbers always are computed with reference to the attenuation of water. The CT number for water is 0, while it is +1000 for bone and −1000 for air on the Hounsfield scale. Furthermore, CT number ranges for bone 800-3000, muscle 35-50, white matter 36-46, gray matter 20-40, blood 13-18, tumors 5-35, fat -100, lungs -150-400, and air -1000.

After obtaining CT numbers this values are converting into a gray scale image, where higher CT numbers are assigned white, lower numbers black, and gray shades between black and white. This assignment is related to the attenuation characteristics of tissues. Bone attenuates more radiation and therefore is assigned white. Air attenuates very little radiation and appears black on image.

1.1.2 Single photon emission computed tomography

Single photon emission computed tomography or SPECT has been widely used in nuclear medicine for several decades. Since the late 1980s and early 1990s SPECT integrates CT and a radioactive tracer to provide complimentary information of anatomy and function for improved diagnostic outcomes. SPECT scans are non-destructive and unlike X-ray CT, which uses radiation from an external X-ray source, SPECT utilizes radiation, from radionuclide-labeled pharmaceuticals (tracers).

Before the SPECT scan, a tracer is injected into a patient by mouth or by injection. The tracer emits gamma rays that can be detected by the CT scanner. Since gamma rays are

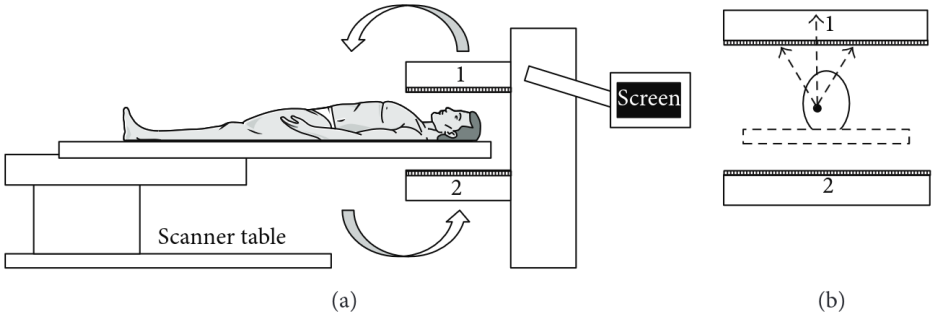

Figure 3. Schematic representation of (a) SPECT scanner along with depiction of (b) gamma detector (1, 2) placement and detection of emissions from a reference point at the time of a brain SPECT scan [4].

normally emitted equally in every direction, it is necessary to use a collimator in front of the detector that allows only the gamma rays emitted in the direction of the detector to be registered. In this way, the collimator defines the direction of the radiation when it is detected by a position-sensitive detector, typically a scintillation camera.

A typical scintillation camera consists of a 0.95-cm-thick, 40-cm-diameter NaI crystal and array of photomultiplier tubes at its back [3]. The detected photons are transformed into visible light (i.e. scintillations), which is converted into electrical signals by the photomultiplier tubes. The magnitudes of the electrical signals are propotional to the energies of the photons. A pulse height analyzer evaluates the energies of the detected photons and accepts only those that fall within a preset energy windows, which is centered at the energy peak of the primary photons. Scattered photons and their adversive effects are rejected. The effectiveness of this scatter rejection depends on the energy resolution of the detector and the width of the energy window. Finally, by moving the detector system completely around the patient, a 360° image is obtained (Fig. 3). Mathematical methods are used to trace the emitted gamma rays back in the direction that they were emitted in order to produce the image.

The radioisotopes typically used in SPECT to label tracers are ^{123}I, ^{131}I, ^{99m}Tc, ^{133}Xe and ^{201}Tl, the half-lives and primary photon energies for these radioisotopes are shown in the Table 1. These isotopes are attracted to specific organs, bones or tissues, which absorb the radioactive material. Once an organ or tissue has absorbed the radioactive material, it produces gamma ray photons, which can be detected by the scanner. A typical example is ^{99m}Tc which emits 140 keV photons (Fig. 4). Various drugs and other chemicals can be labeled with these isotopes.

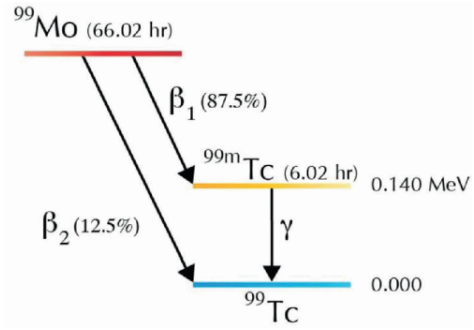

Figure 4. Technetium-99m decay scheme [5].

Radionuclide	Half-life	Emission energy, keV
Iodine-123	13.2 h	159
Iodine-131	8.02 d	364
Technetium-99m	6 h	140
Xenon-133	5.25 d	81, 161
Thallium-201	73 h	∼ 72

Table 1. Radionuclides commonly used in SPECT

1.1.3 SPECT/CT

The SPECT/CT scanner combines the framework of the CT scan with the functional information provided by SPECT. The images from each scan are then fused together providing highly accurate anatomical detail in 3D, allowing medical specialists to more accurately pinpoint the exact location of any abnormality.

SPECT/CT offers several advantages over using these systems independently:

- SPECT/CT offers more precise localization and characterization of functional findings;
- The combination of SPECT and CT leads to improved diagnostic accuracy, which is associated with greater diagnostic confidence and better inter-specialty communication;
- CT coregistration in SPECT/CT is based on the attenuation correction capabilities of CT, which improves quality in SPECT images;
- SPECT/CT offers the opportunity to add true diagnostic information derived from CT imaging.

These advantages make SPECT/CT a powerful tool in various clinical domains, including oncology, endocrinology, orthopaedics, paediatrics, and cardiology.

1.2 Dose safe limits

Despite its many benefits, the use of SPECT/CT for scans is associated with increased radiation exposure for patients due to the combined radiopharmaceutical dose from SPECT and radiation dose from the CT.

The effective dose (E) is a useful measure that can be used to assess the radiation dose of SPECT/CT scans. The International Commission on Radiological Protection (ICRP) recommends using E for radiological protection planning and optimization, demonstrating dose limits for regulatory purposes, and comparing typical doses from examinations involving ionizing radiation [6]. Notably, E enables the comparison and evaluation of radiation from various sources, including SPECT/CT scans. Effectively, it improves understanding of SPECT/CT by displaying the contribution of each modality to the overall dose received by patients.

The patient effective dose associated with a SPECT/CT procedure was calculated as the sum of the effective dose from the radiopharmaceutical administered and the effective doses from the CT scan.

The effective dose due to radiopharmaceutical administration (E_{RF}) can be determined from the average organ-absorbed doses ($D_{T,R}$) as follows [7]:

$$E_{RF} = \sum_T w_T \sum_R w_R D_{T,R}, \tag{3}$$

where w_T is the tissue-weighting factor for tissue T, accounting for different organ radiosensitivities. Tissue-weighting factor values are updated by the ICRP based on epidemiological evidence of cancer induction and radiation-induced inherited effects in exposed populations, these factors are shown in Table 2. The coefficient w_R depends on the type of radiation considered and is associated with the higher relative biological efficiency of high linear energy transfer (LET) radiation with respect to low LET radiation. Its value is 1 for photons and electrons. $D_{T,R}$ refers to the average of both men and women organ-absorbed doses. The $D_{T,R}$ values can be extracted, for example, from the ICRP Radiation dose to patients from radiopharmaceuticals [8].

The effective dose due to CT scan (E_{CT}) can be calculated by the Dose-Length Product (DLP) method i.e. [7]:

$$E_{CT} = k \cdot DLP, \tag{4}$$

where DLP is a dose descriptor that depends on irradiated length, acquisition parameters and

Tissue	w_T
Bone-marrow(red)	0.12
Lung	0.12
Colon	0.12
Stomach	0.12
Breast	0.12
Gonads	0.08
Bladder	0.04
Liver	0.04
Esophagus	0.04
Thyroid	0.04
Skin	0.01
Bone surface	0.01
Brain	0.01
Salivary glands	0.01
All other tissues	0.12

Table 2. Recommended tissue-weighting factors from ICRP103 publication [6].

CT design. The equipment provided the DLP value for each scan, k is a conversion coefficient that is solely dependent on the anatomical region scanned, and these values have been published in [6].

The dose limits provided by ICRP recommendations are for medical personnel or workers in a nuclear installation wearing a personal dosimeter – a whole-body dose rate of 20 mSv/yr, or about 2.3 μSv/h. If only parts of the body such as the skin, the hands or the feet are exposed, 500 mSv/yr (57 μSv/h) are still considered safe.

The ICRP dose limits for public - a whole-body effective dose rate is 1 mSv/yr. And for skin the equivalent dose is 50 mSv/yr.

1.3 Interaction of photons with matter

SPECT/CT imaging technique is based on the certain physical processes of interaction of photons with matter.

The behavior of photons in matter is completely different from that of charged particles. In particular, the photon's lack of an electric charge makes impossible the many inelastic collision with atomic electrons so characteristic of charged particles. For this kind of radiation the most important mechanism of interaction are

- Photoelectric effect,
- Compton and Rayleigh scattering,
- Pair production.

The Rayleigh scattering does not change the energy of the incident photons and consequently has no direct consequence on the detection. The occurrence of the other three types of interactions depends on the atomic number of the element and the energy of the incident photon (Figure 5).

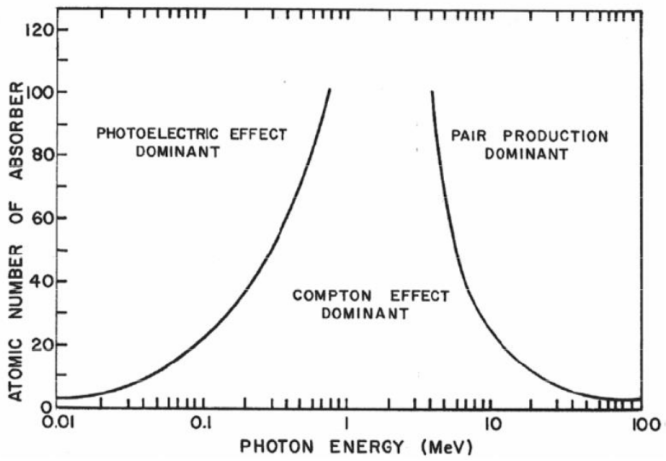

Figure 5. Relative importance of the processes of interaction of photons with matter as a function of their energy and the medium composition [9].

1.3.1 Photoelectric effect

This process is is characterized by the whole energy of the incident photon ($E = h\nu_0$) is transferred to an internal electron of an atom of the absorbing material (Figure 6). The energy of the incident photon is totally absorbed by the electron which is then ejected (photoelectron) with a kinetic energy depending on the energy of the incident photon and the binding energy of the corresponding electronic shell (or sub-shell). This phenomenon is dependent on the target atom and its cross-section has a strong dependence on the atomic number of the element as Z^5.

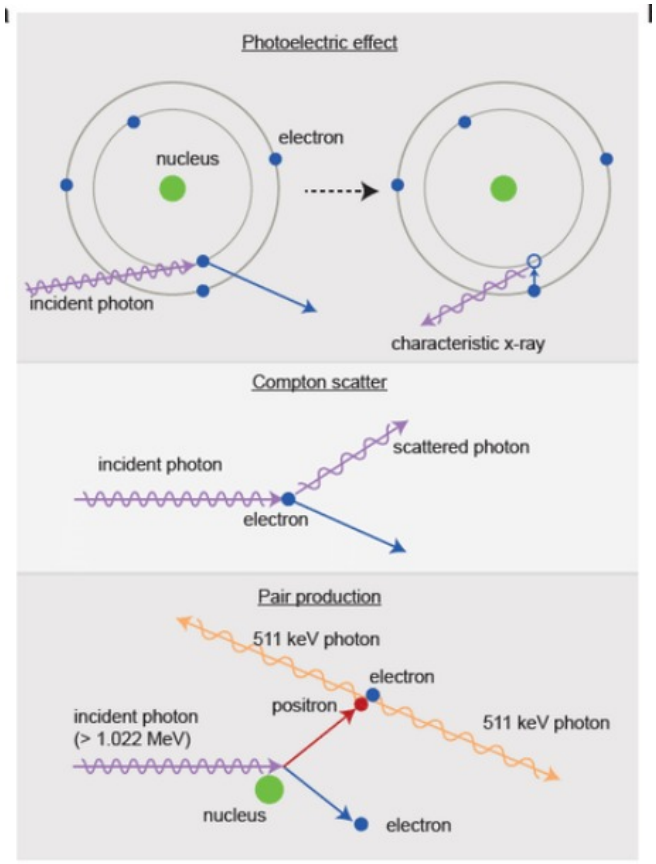

Figure 6. Diagrams of the main processes of interaction of photons with matter.

1.3.2 Compton scattering

This process corresponds to the inelastic scattering of the incident photon onto an electron of an atom (Figure 6). During this interaction, the incident photon is scattered at an angle with respect to its original direction and yields part of its energy to the electron. The latter is then ejected from the atom with kinetic energy and some angle with respect to the incident direction. This type of interaction is little dependent on the environment, and evolves in Z/A.

1.3.3 Pair production

In this process, the photon energy is converted into a positron-electron pair under the action of the intense Coulomb field around the atom nucleus. This process is energetically possible only if the incident energy is greater than the sum of the masses of the electron and the positron, i.e $E_{threshold} = 2m_e c^2 = 1.022$ MeV (Figure 6). The positron emitted during this process rapidly interacts with surrounding medium and annihilates with an electron, producing two 511 keV photons emitted at 2π from each other. The higher both the atomic number of the medium, proportional to Z^2, and the energy of the photons ($h\nu_0 > E_{threshold}$), the higher the probability of producing pairs. This phenomenon is useful, for example, in PET imaging.

1.4 Monte-Carlo method

The Monte Carlo method is a statistical technique which is capable of simulating a mathematical or physical experiment on a computer. In mathematics, it can provide the expectation value of functions and evaluate integrals; in science and engineering, it is capable of simulating complex problems which are comprised of various random processes with known or assumed probability density functions. To be able to simulate the random process, i.e., sample from a probability function for an event, it uses random numbers or pseudo-random numbers. Just like any statistical process, the Monte Carlo method requires repetition to achieve a small relative uncertainty, and therefore, may necessitate impractically large simulation times. To overcome this difficulty, parallel algorithms and variance reduction techniques are needed.

Monte Carlo can be used to simulate a random walk process (such as the interaction of radiation with materials) and is particularly useful for complex problems. The individual probabilistic events that comprise a particle history from birth to death are simulated sequentially, but particle histories can be simulated in parallel. The probability distributions governing these events are statistically sampled to describe the total phenomenon.

1.5 MCNP for modelling radiation transport in matter

Monte Carlo N-Particle Transport (MCNP) [10] is a general-purpose, continuous-energy, generalized-geometry, time-dependent, Monte Carlo radiation transport code designed to track many particle types over broad ranges of energies and is developed by Los Alamos National Laboratory.

The MCNP code treats neutrons and photons as particles moving in a straight line between collisions. Figure 7 represents the random history of a neutron incident on a slab of material that can undergo fission. Numbers between 0 and 1 are selected randomly to determine what (if any) and where interaction takes place, based on the rules (physics) and probabilities (nuclear data) governing the processes and materials involved. In this particular example, a neutron collision occurs at event 1. The neutron is scattered in the direction shown, which is selected randomly from the physical scattering distribution. A photon is also produced and is temporarily stored, or banked, for later analysis. At event 2, fission occurs, resulting in the termination of the incoming neutron and the birth of two outgoing neutrons and one photon. One neutron and the photon are banked for later analysis. The first fission neutron is captured at event 3 and

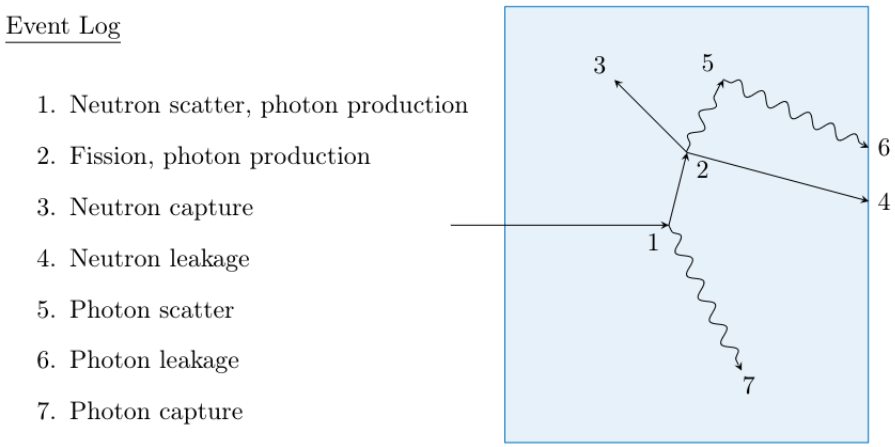

Figure 7. Various particle random walks. The zigzag lines are used to represent the moving of photons in the MCNP user manual, but the MCNP code treats a photon movement as a straight line between collisions [10].

terminated. The banked neutron is now retrieved and, by random sampling, leaks out of the slab at event 4. The fission-produced photon has a collision at event 5 and leaks out at event 6. The remaining photon generated at event 1 is now followed with a capture at event 7. Note that the MCNP code retrieves banked particles such that the last particle stored in the bank is taken out first (i. e., last-in-first-out stack). This neutron history is now complete. As more and more such histories are followed, the neutron and photon distributions become better known. The quantities of interest (whatever the user requests) are tallied, along with estimates of the statistical precision (uncertainty) of the results.

2 Results

Based on the project objective – to build the dependency of dose rate vs distance a preclinical SPECT/CT scanner was simulated with MCNP Monte-Carlo code. The geometry of this tomograph is shown in Fig. 8. The center of coordinates in the simulated system is placed inside the phantom mouse model heart, which is in the center of the animal. So, all distances are relative to the (0,0,0) point. Point detectors have been placed along the x-axis (Fig. 8 (c)). And the lead protection wall was placed in 33 cm point along the x-axis.

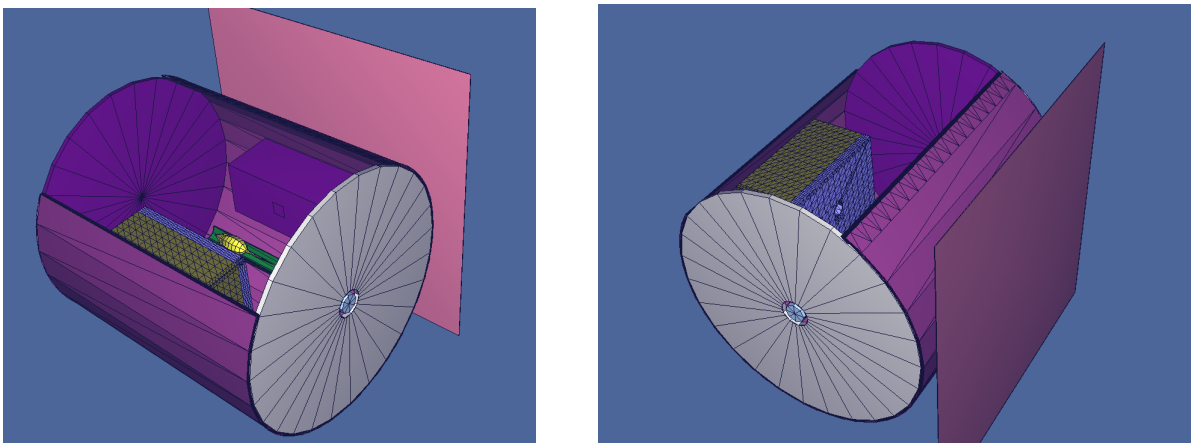

(a) (b)

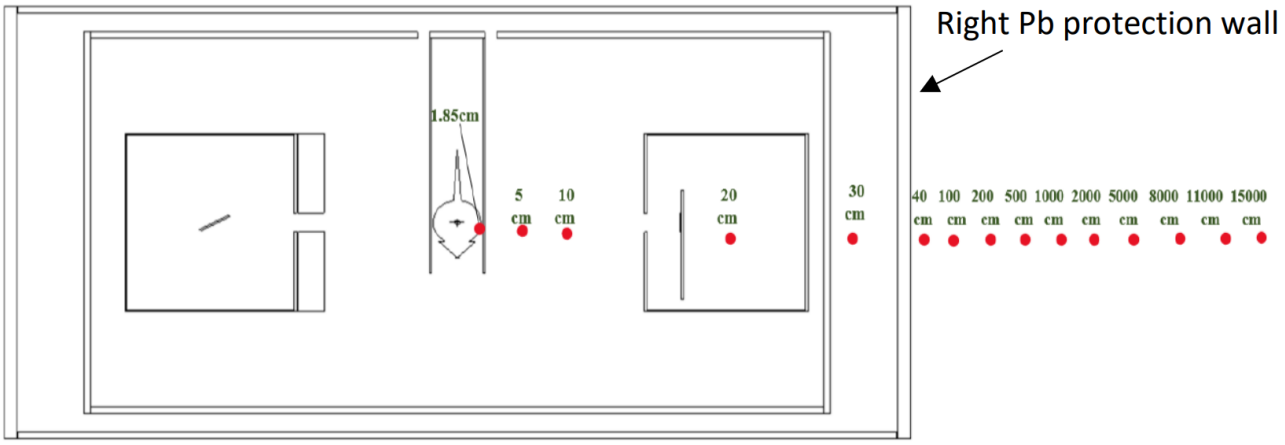

(c)

Figure 8. The geometry of SPECT/CT scanner. (a) and (b) representing a 3D view, (c) - the layout of the point detectors.

2.1 CT

For computed tomography X-ray scan configuration, the W anode X-ray tube was approximated with a point source placed at 1 mm in front of the imaginary tungsten anode. This source emits photons in the direction of the phantom inside a 20-degree cone, whose axis coincides with the x-axis. The tungsten emission spectrum was calculated using interpolating polynomials (TASMIP) for 120 kV without any filtration [11] (Figure 8).

The measurements of the particle fluence in the places of interest are achieved with the use of a point detector. The results are obtained in part./cm^{-2} units.

To calculate the quantity of photons emitted by the source the following approximation was chosen. Since the tube of W is operating at 120 kV and 350 μA, that means, 1 A = 1

C/s $= 6.241 \cdot 10^{18}\ e^-/s$, 350 μA $= 2.184 \cdot 10^{15}\ e^-/s \longrightarrow 7.862 \cdot 10^{18}\ e^-/h$. From all electrons impacting the anode only the 1 % produce X-ray photons; the rest is lost in heating up the target. That is, the efficiency of the tube at producing X-ray is about 1 %. In this way the amount of photons emitted by the source is $7.862 \cdot 10^{16}$ photons/h. This multiplies the results and pSv*part$\longrightarrow$ pSv/h. Finally multiplying by 10^{-6} convert from pSv/h to μSv/h.

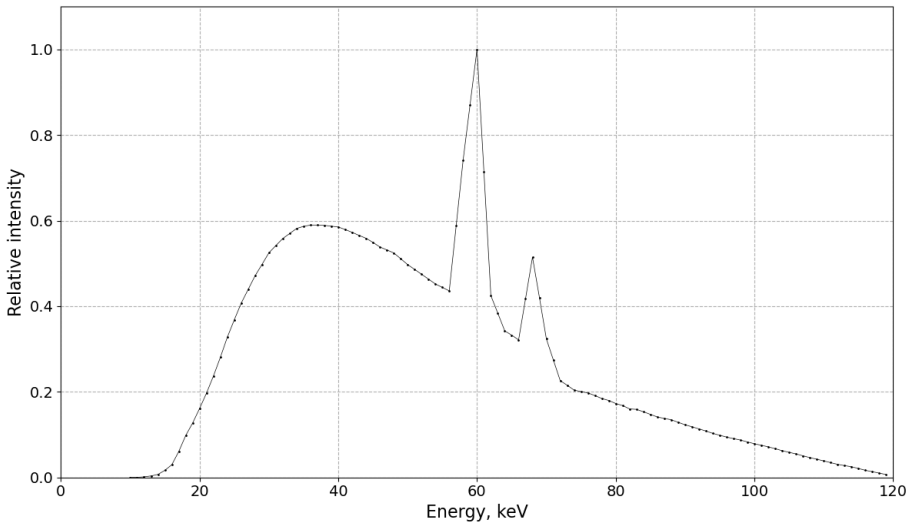

Figure 9. X-ray tube spectrum with tungsten cathode.

Monte-Carlo simulation was performed for 10^6 photons from X-ray source. The lead protection was varied from 0 to 2 cm. And results for dependency of dose rate vs distance is shown in Figure 10.

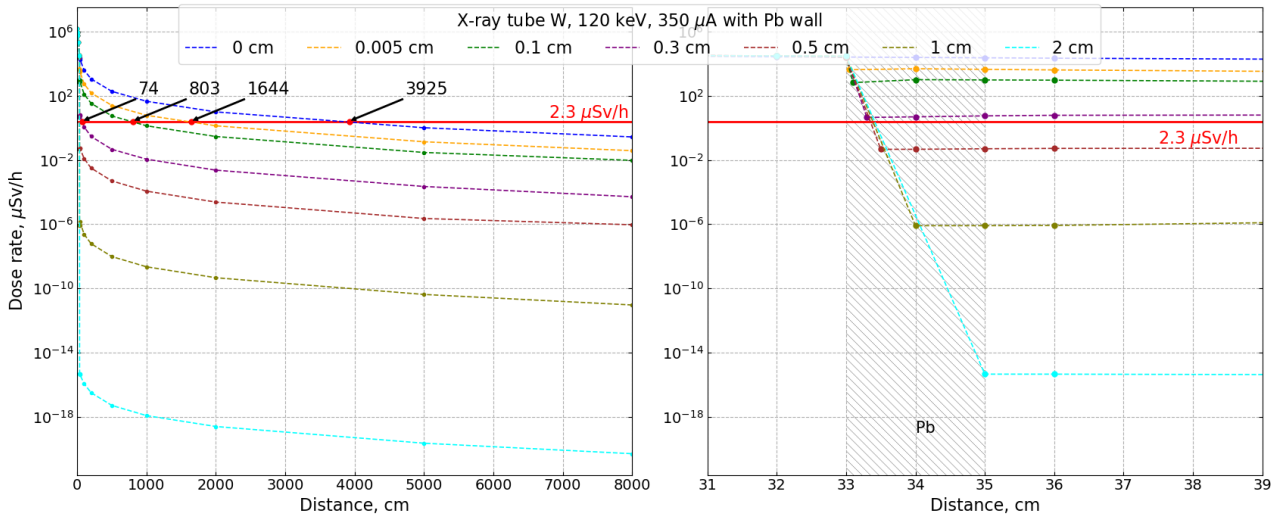

Figure 10. Dependency of dose rate vs distance from X-ray source used in CT scan. Arrows with numbers are representing safe distance in cm after corresponding lead protection, for example 803 cm after 0.1 cm Pb wall. Hatching lines shows the area where Pb wall thickness was varied.

For a preclinical tomograph with the characteristics of the simulated one, in the absence of a protective Pb wall, being at a distance less than 3925 cm is not safe. For great radiation protection is a Pb wall with thickness at least of 0.5 cm is required to reduce the dose rate that can affect the worker.

2.2 SPECT

For the SPECT configuration, a point source (tracer) of different isotopes was placed in the center of coordinates (0,0,0). This source emits isotropically in 4π with a photon emission energy (for example 140 keV for ^{99m}Tc) and has an activity depends on isotope(10 MBq for ^{99m}Tc).

The dose conversion is made by the following way. For ^{99m}Tc: 10 MBq $= 1 \cdot 10^7$ desint./s (this source emits 1 photon in each desintegration) $= 1 \cdot 10^7$ photons/s $= 3.6 \cdot 10^{10}$ photons/h. And multiplying this value by $1 \cdot 10^{-6}$ convert from pSv/h to μSv/h.

Monte-Carlo simulation was performed for 10^6 photons from ^{99m}Tc source. The lead protection was varied from 0 to 1 cm. And results for dependency of dose rate vs distance is shown in Figure 11.

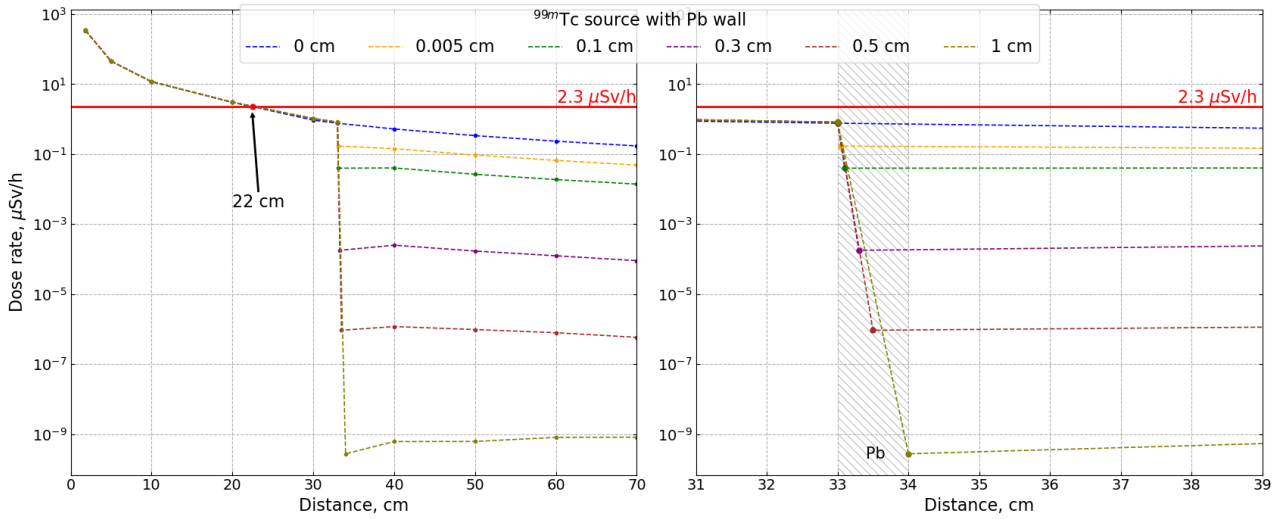

Figure 11. Dependency of dose rate vs distance from ^{99m}Tc source used in SPECT scan. Hatching lines shows the area where Pb wall thickness was varied.

For the SPECT scan with ^{99m}Tc source the safe dose is achieved at 22 cm form source position before lead protection. That's means for a preclinical tomograph with the characteristics of the simulated one the absence of Pb protection wall can't affect the personnel.

For the ^{131}I tracer with the activity of 74 MBq and 364 keV photon energy the dose conversion is made by the following way: 74 MBq $= 7.4 \cdot 10^7$ desint./s $= 7.4 \cdot 10^7$ photons/s $= 26.6 \cdot 10^{10}$ photons/h. Multiplication of this value by $1 \cdot 10^{-6}$ convert from pSv/h to μSv/h.

Simulation was performed for 10^6 photons from ^{131}I source. The lead protection was varied from 0 to 1 cm. And results for dependency of dose rate vs distance is shown in Figure 12 and demonstrates quite different results by comparison with ^{99m}Tc source.

The safe dose is achieved after the distance of 92 cm without lead protection wall for such SPECT scan with ^{131}I source. For Pb thicknesses as 0.005 cm, 0.1 cm, 0.3 cm, 0.5 cm, 1 cm those distances are 84 cm, 77 cm, 58 cm, 44 cm respectively. That's means for a preclinical SPECT scan with the ^{131}I tracker and characteristics as CT, Pb wall with thickness at least of 1 cm is required to reduce the dose rate that can affect the worker.

For the ^{201}Tl tracer with the activity of 55.5 MBq and 70 keV photon energy the dose conversion is: 55.5 MBq $= 5.6 \cdot 10^7$ desint./s $= 5.6 \cdot 10^7$ photons/s $= 20 \cdot 10^{10}$ photons/h. Multiplication of this value by $1 \cdot 10^{-6}$ convert from pSv/h to μSv/h.

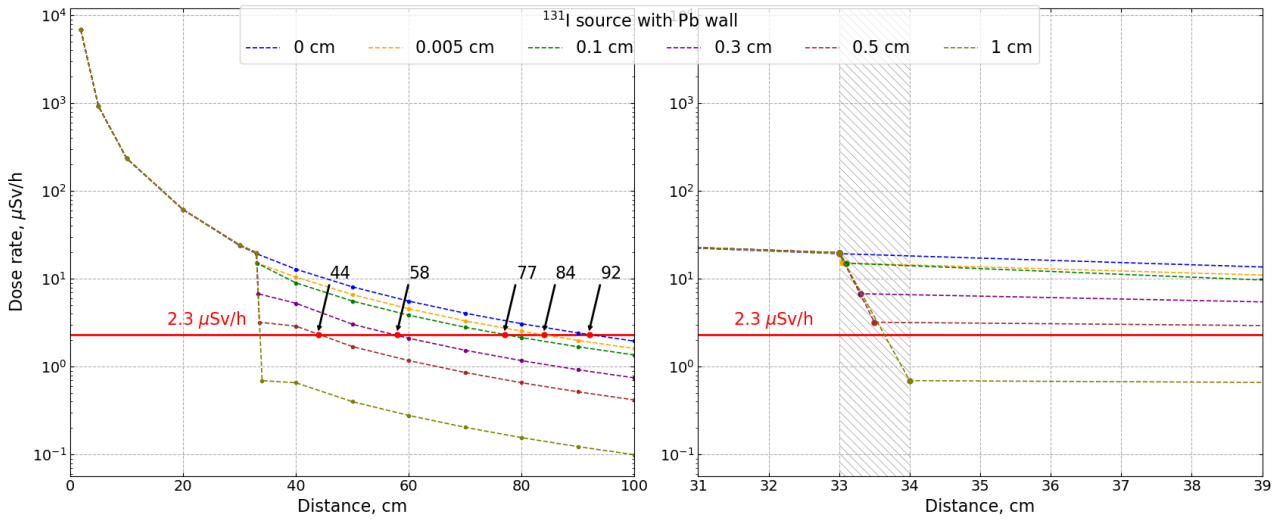

Figure 12. Dependency of dose rate vs distance from ^{131}I source used in SPECT scan. Arrows with numbers are representing safe distance in cm after corresponding lead protection. Hatching lines shows the area where Pb wall thickness was varied.

Simulation was performed as the previous one for 10^6 photons from ^{201}Tl source. The lead protection again was varied from 0 to 1 cm. And results for dependency of dose rate vs distance is shown in Figure 13 and illustrates result is quite similar as for ^{99m}Tc source.

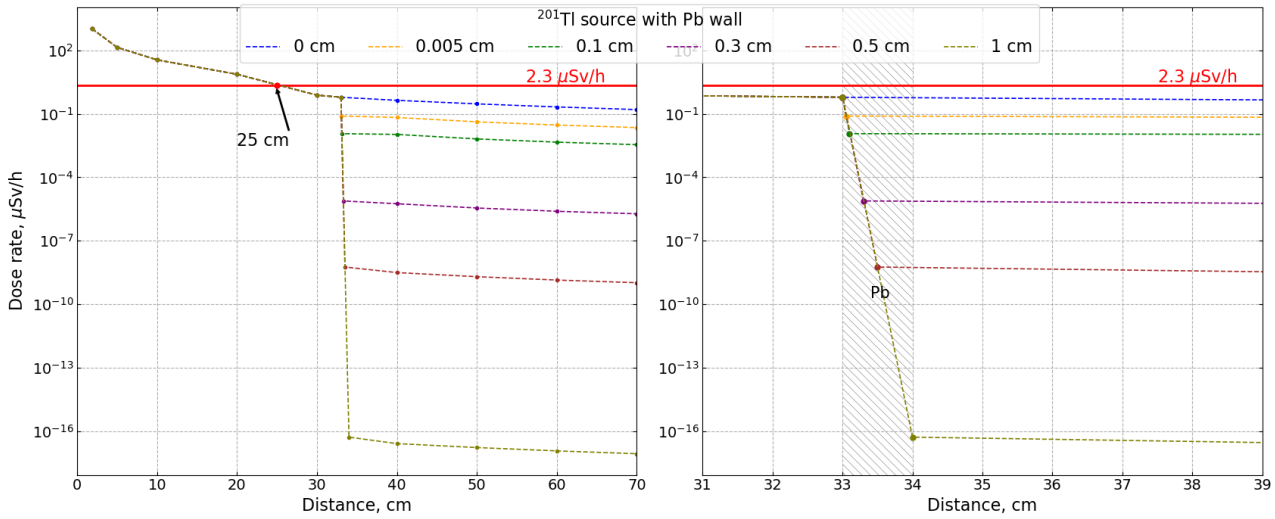

Figure 13. Dependency of dose rate vs distance from ^{201}Tl source used in SPECT scan. Hatching lines shows the area where Pb wall thickness was varied.

For such configuration of SPECT scan with ^{201}Tl source the safe dose is achieved at 25 cm point form source position before lead protection. In that case Pb protection is not necessary.

Conclusions

Since the advent of CT scanners, advances in technology and capabilities have enabled many new clinical applications to be rapidly implemented. One such application is the SPECT/CT hybrid imaging system, which continues to grow in popularity in nuclear medicine/cardiology facilities.

A SPECT/CT combination allows for the sequential collection of anatomic/molecular data while minimizing patient position changes, enhancing attenuation correction and providing anatomic images that are inherently coregistered.

While there are clear advantages to this technology, recent advances in hybrid imaging, such as combining SPECT with CT systems, lead to higher patient exposure levels, increased occupational hazard from scattered radiation, and the need for increased shielding within a nuclear medicine department.

In this project the MCNP code system based on the Monte Carlo method used to simulate the interaction of radiation with matter, to study radiation shielding for the preclinical SPECT/CT scanner.

For computed tomography X-ray scan configuration with the W anode the absence of the protective Pb wall, being at a distance less than 3925 cm is not safe. For necessary radiation protection is a Pb wall with thickness at least of 0.5 cm is required to reduce the dose rate that can affect the worker.

For the SPECT configuration simulation a tracer with different isotopes was used. The radiation exposure from the 10 MBq ^{99m}Tc and 55.5 MBq ^{201}Tl with photon energy of 140 keV and 70 keV respectively becomes safe before lead shielding. In these cases Pb protection is not required and dose rate comply with the radiation protection requirements demanded at ICRP.

The effective dose from ^{121}I with activity of 74 MBq and photon energy of 364 keV an order of magnitude more than the previous trackers. Therefore, the radiation exposure will have a more noticeable effect on personnel after lead protection. It's highly necessary for using lead protection at least with thickness of 1 cm.

Monte Carlo simulation technique, such as the MCNP code system, is very useful tool for simulation the interaction of radiation with matter, especially for studying radiation shielding in medical applications. In this project, it was shown that with the Monte Carlo simulation, it is possible to estimate the radiation shielding parameters of the medical device for example the preclinical SPECT/CT scanner.

References

[1] E. Seeram. *Dose Optimization in Digital Radiography and Computed Tomography: An Essential Guide*. Springer International Publishing, 2023. ISBN: 9783031228711.

[2] *X-RAY COMPUTED TOMOGRAPHY: A BRIEF INTRODUCTION*. URL: https://imaging.rigaku.com/learning/x-ray-computed-tomography-brief-introduction.

[3] BM Tsui. "The AAPM/RSNA physics tutorial for residents. Physics of SPECT". In: *RadioGraphics* 16.1 (1996). PMID: 10946698, pp. 173–183. DOI: 10.1148/radiographics.16.1.173.

[4] Abishek Arora and Neeta Bhagat. "Insight into the Molecular Imaging of Alzheimer's Disease". In: *International Journal of Biomedical Imaging* 2016 (2016).

[5] *Basics of Nuclear Medicine Physics and Radiation Safety*. URL: https://radiologykey.com/basics-of-nuclear-medicine-physics-and-radiation-safety.

[6] Monty W. Charles. "ICRP Publication 103: Recommendations of the ICRP†". In: *Radiation Protection Dosimetry* 129.4 (May 2008), pp. 500–507.

[7] Carlos Montes et al. "Estimation of the total effective dose from low-dose CT scans and radiopharmaceutical administrations delivered to patients undergoing SPECT/CT explorations". In: *Annals of nuclear medicine* 27 (Apr. 2013).

[8] S Mattsson et al. "Radiation dose to patients from radiopharmaceuticals: A compendium of current information related to frequently used substances". en. In: *Ann. ICRP* 44.2 Suppl (July 2015), pp. 7–321.

[9] G. M. Volkoff. "The Atomic Nucleus. Robley D. Evans. McGraw-Hill, New York, 1955. xv+ 972 pp." In: *Science* 123.3197 (1956), pp. 592–593.

[10] Joel Aaron Kulesza et al. *MCNP® Code Version 6.3.0 Theory & User Manual*. Tech. rep. LA-UR-22-30006, Rev. 1. Los Alamos, NM, USA: Los Alamos National Laboratory, Sept. 2022.

[11] *TASMIP Spectra Calculator*. URL: https://solutioinsilico.com/medical-physics/applications/tasmip-app.php.

Acknowledgments

I would like to express my special thanks to my supervisor Dr Antonio Leyva Fabelo for his time and efforts he provided throughout the project. Your useful advice and suggestions were really helpful to me during the project's completion. In this aspect, I am really grateful to you.